ELSEVIER

Ceramics International 31 (2005) 543–553

CERAMICS
INTERNATIONAL

www.elsevier.com/locate/ceramint

Spark-plasma-sintered $ZrO_2(Y_2O_3)$-$BaCrO_4$ self-lubricating composites for high temperature tribological applications

J.H. Ouyang*, S. Sasaki, T. Murakami, K. Umeda

Tribology Group, National Institute of Advanced Industrial Science and Technology (AIST),
1-2 Namiki, Tsukuba, Ibaraki 305-8564, Japan

Received 2 April 2004; received in revised form 25 May 2004; accepted 20 June 2004
Available online 11 September 2004

Abstract

Self-lubricating $ZrO_2(Y_2O_3)$-$BaCrO_4$ composites have been fabricated by spark plasma sintering by tailoring the composition. The friction and wear properties in dry sliding against an alumina ball were evaluated by using a SRV friction and wear tester from room temperature to 800 °C. The composites exhibit distinct improvements in effectively reducing friction and wear over a wide temperature range, as compared to the unmodified $ZrO_2(Y_2O_3)$ ceramics. The $ZrO_2(Y_2O_3)$-50$BaCrO_4$ composite exhibits a friction coefficient of 0.38–0.55 and a wear rate of 1.44×10^{-5} to 5.35×10^{-5} mm^3/Nm up to 800 °C. Surface brittle fracture is considered as the dominating wear mechanism of the composite at room temperature. At elevated temperatures, a self-lubricating $BaCrO_4$ fine-grain layer forms on the worn surfaces, and is partially transferred to the counterface to reduce the friction and wear. The plastic deformation of $BaCrO_4$ at elevated temperatures plays an important role to form a well-covered $BaCrO_4$ fine-grain layer at the tribo-contact regions. The effect of sintering temperature on microstructure and tribological properties of the self-lubricating $ZrO_2(Y_2O_3)$-50$BaCrO_4$ composite has been discussed.

Keywords: C. Friction; D. ZrO_2; D. Y_2O_3; $BaCrO_4$; Self-lubricating composite; High temperatures; Wear

1. Introduction

Research on self-lubricating ceramic matrix composites (CMCs) has been initiated as a response to the requirements for greater efficiency in all types of engines that uses ceramic components at extreme temperatures [1–6]. In recent years, the increasing potential for the use of ZrO_2 ceramics as the hot-section components in advanced engines and gas turbines, and wear-resistant sliding components in lubrication and seal systems has focused a great attention on these materials [5,7]. As the friction of unlubricated ZrO_2 ceramic surfaces at elevated temperatures is usually high and unacceptable, it is necessary to find ways of effectively lubricating ZrO_2 ceramics if they are to be used extensively to extreme temperature conditions.

A series of self-lubricating composites based on solid lubricants of silver and CaF_2 or CaF_2/BaF_2 eutectic were developed by plasma spraying and powder metallurgy methods [1–9]. These composites consist in a wear-resistant matrix (Ni-Cr-Cr_3C_2, Ni-Cr-Cr_2O_3, Al_2O_3 or ZrO_2) combined with silver and CaF_2 or CaF_2/BaF_2 eutectic solid lubricants [1–9]. A metal-bonded chrome oxide doped with silver and BaF_2/CaF_2 eutectic lubricants provided good friction and wear properties over a wide temperature range [2,8]. A self-lubricating alumina matrix composite with Ag/CaF_2 synthesized by a powder metallurgy method can provide low friction and wear over a temperature range of 300–750 °C [3]. To date, only a limited amount of experiments have been done on high-temperature lubrication of ZrO_2 ceramics. The friction and wear coefficients of ZrO_2-CaF_2 coatings doped with and without silver additives showed that both coating combinations had fairly high wear rates at room temperature, but wear rates were much lower for the ZrO_2-CaF_2 coating at 650 °C as compared to the

---

* Corresponding author. Tel.: +81 29 8617844; fax: +81 29 8617844.
E-mail address: jiahu-ouyang@aist.go.jp (J.H. Ouyang).

0272-8842/$30.00 © 2004 Elsevier Ltd and Techna Group S.r.l. All rights reserved.
doi:10.1016/j.ceramint.2004.06.020

Table 1
Chemical compositions, densities and hardness of $ZrO_2(Y_2O_3)$ matrix composites with various amounts of $BaCrO_4$ additive

Materials	Compositions (wt.%)	SPS sintering parameters	Vickers hardness (HV_1)	Density (g/cm^3)
YPSZ	$ZrO_2(Y_2O_3)$	1500 °C, 10 min, 40 MPa	1260	5.73
ZB1	$70ZrO_2(Y_2O_3)$, $30BaCrO_4$	1100 °C, 5 min, 40 MPa	485	5.12
ZB2	$50ZrO_2(Y_2O_3)$, $50BaCrO_4$	1100 °C, 5 min, 40 MPa	426	4.99

unmodified ZrO_2 coatings [1]. The addition of silver did not have a beneficial effect in improving friction and wear in sliding contact with two flat nickel base superalloy rub blocks [1]. A low-pressure plasma-sprayed ZrO_2-CaF_2 coating exhibited low friction and wear in sliding against an alumina ball during the wear test runs at 600–700 °C [4]. We have developed a self-lubricating $ZrO_2(Y_2O_3)$ matrix composite coating doped with CaF_2/Ag_2O lubricants synthesized by low-pressure plasma-spraying. It provided low friction and wear against an alumina ball over a temperature range of 300–700 °C [5]. However, excessive material transfer and plastic deformation leads to high friction and wear of the coatings at 800 °C.

In recent years, the ternary compounds ($ACrO_4$ and ACr_2O_4, A = Ba, Sr, and Ca) between alkaline earth metal oxides and chromium sesquioxide have been investigated as solid lubricants for ceramic matrix composites [10,11]. The addition of 50 vol.% $BaCrO_4$ into a $ZrO_2(Y_2O_3)$ matrix coating produced by low-pressure plasma spraying effectively reduced friction and wear at above 300 °C due to the formation of a lubricating film [10]. Tribological properties of spark-plasma-sintered (SPS) ceramics such as $BaCrO_4$, $BaCr_2O_4$, Al_2O_3-$BaCrO_4$, Al_2O_3-$BaCrO_4$-Ag and Al_2O_3-$BaCrO_4$-$BaCr_2O_4$ have been evaluated with a reciprocating wear tester from room temperature to 1300 °C [11]. The results have demonstrated that $BaCrO_4$ possesses a good self-lubricating capacity at high temperatures, and has adequate thermo-chemistry and low shear strength at elevated temperatures. Al_2O_3-50 vol.% $BaCrO_4$ composites sintered by SPS exhibited excellent friction and wear characteristics from room temperature to 1000 °C as compared to unmodified alumina [11]. A plasma-sprayed composite coating with combinations of CaF_2, BaF_2 and Cr_2O_3 powders also exhibited excellent friction properties, with μ = 0.20–0.30 in a wide temperature range of 300–900 °C. The low friction coefficient was attributed to the coexistence of CaF_2 and $BaCrO_4$, which were formed by the tribo-chemical reaction on the worn surfaces at high temperatures [12].

In this paper, spark plasma sintering (SPS) is employed to synthesize self-lubricating $ZrO_2(Y_2O_3)$-$BaCrO_4$ composites by tailoring the composition and by adjusting the sintering temperature. Further studies are carried out to evaluate the effects of sintering temperature and the $BaCrO_4$ content and to identify the lubrication mechanisms of the composites using a SRV friction and wear tester against an alumina ball up to 800 °C.

2. Experimental procedure

Self-lubricating $ZrO_2(Y_2O_3)$-$BaCrO_4$ composites were fabricated by a SPS apparatus (SPS-1050, Sumitomo Coal Mining Co. Ltd., Japan). The powder materials used in this investigation was 8 wt.% Y_2O_3 partially stabilized ZrO_2 (YPSZ) and $BaCrO_4$. The powders have a particle size in the range of 1–5 μm. These powders were blended and ball-milled in proper ratios by weight to form composite powders. The cold compaction of the mixed powder was carried out in a graphite mold (inner diameter 20 mm, outer diameter 50 mm) at a pressure of 40 MPa to produce cylindrical slugs. Following cold compaction, ceramic matrix composites of ZrO_2-$BaCrO_4$ were fabricated by SPS. For a comparative wear test study, specimens of $ZrO_2(Y_2O_3)$ ceramics doped with and without 30 wt.% $BaCrO_4$ additives are also spark-plasma-sintered. The sintering was carried out in a graphite mold at 1050 to 1500 °C of temperature, 40 MPa of pressure, 5 to 10 min of holding time, and 50 °C/min of heating rate. Table 1 lists the chemical compositions, densities and hardness of $ZrO_2(Y_2O_3)$ matrix composites with various amounts of $BaCrO_4$ additive. Table 2 describes the effects of SPS sintering temperature on the hardness and density of the $ZrO_2(Y_2O_3)$-$50BaCrO_4$ composites.

Densities of the sintered samples were determined by the Archimedes method. The surfaces and cross sections of the sintered samples were ground and polished for microstructural observations. The microstructure and chemical composition of the $ZrO_2(Y_2O_3)$ matrix composites were characterized by using a scanning electron microscope (SEM) equipped with energy dispersive X-ray (EDX) analysis

Table 2
Effects of SPS sintering parameters on the hardness and density of the $ZrO_2(Y_2O_3)$-$50BaCrO_4$ composites

Materials	Compositions (wt.%)	SPS sintering parameters	Vickers hardness (HV_1)	Density (g/cm^3)
ZB21	$50ZrO_2(Y_2O_3)$, $50BaCrO_4$	1050 °C, 5 min, 40 MPa	408	4.94
ZB2	$50ZrO_2(Y_2O_3)$, $50BaCrO_4$	1100 °C, 5 min, 40 MPa	426	4.99
ZB23	$50ZrO_2(Y_2O_3)$, $50BaCrO_4$	1150 °C, 5 min, 40 MPa	451	5.03
ZB24	$50ZrO_2(Y_2O_3)$, $50BaCrO_4$	1300 °C, 5 min, 40 MPa	389	4.95

system and operated at 10 kV. The crystal structure of the composites was determined by X-ray diffractometer (XRD) with a 40 kV operating voltage and Cu Ka radiation. A scanning program with a 2θ scanning rate of $2^\circ\ \mathrm{min}^{-1}$ was employed to determine the peak positions of phases occurring in the range of $20 < 2\theta < 80^\circ$. The wear tracks and wear debris sticking on the wear scars were analyzed using a laser Raman spectroscopy (Renishaw 2000 system) to identify the possible structural modifications generated during the wear process. Raman spectra were measured in the wave number ranging from 100 to 1200 cm^{-1} at the operating power of 25 mW excited by the 514.5 nm lights from an argon ion laser. The laser beam was focused through a standard 20× objective of an optical microscope on the samples. Specimens were indented using a Vickers hardness tester with a load of 9.8 N on polished surfaces or cross-sections.

The wear tests of the composites were performed by using a standard SRV friction and wear tester (Schwingungs Reibung und Verschleiss, Optimol Instruments Prueftechnik GmbH, Germany) with reciprocating motion against a 10 mm alumina ball. The dimensions of the composites for wear tests were 20 mm in diameter and 8 mm in thickness. The chemical composition (wt.%) of alumina ball is 99.5 Al_2O_3, 0.20 SiO_2, 0.14 MgO, 0.09 CaO, 0.03 Fe_2O_3 and 0.03 Na_2O. The alumina balls were used in the as-received condition with a surface roughness of 0.02 μm (Ra), a hardness of 16.5 GPa and a density of 3.95 g/cm^3. Before wear test, the spark-plasma-sintered composites were carefully polished to obtain a surface roughness of 0.2 μm (Ra). The detailed description of a SRV tester is available from previous papers [4,5,10]. Test temperatures can be controlled by a thermocouple up to 900 °C. The wear parameters were given as 10–30 N load, 10 Hz frequency, from room temperature to 800 °C, 1 mm stroke and 1 h test duration. The test atmosphere was air with a relative humidity of 40% at room temperature. The wear depth profiles of all the wear tracks were examined by using a surface profilometer. A set of equally spaced depth profiles covering the whole wear track area was used to evaluate the volumetric wear of the composite. The wear volume of alumina removed from the coupled ball was acquired by using a geometric technique, measuring the diameter of the wear scar formed on the ball with an optical microscope and assuming that the wear scar is perfectly circular and flat in order to simplify the calculations. Wear was expressed as wear rate which relates volumetric wear to sliding distance and to load. The morphology and the chemical compositions of the worn surfaces on the composites and the counterfaces were examined by SEM equipped with EDX to find the lubrication mechanisms.

3. Results

3.1. Density, hardness and structural analysis of the $ZrO_2(Y_2O_3)$-$BaCrO_4$ composites

The $ZrO_2(Y_2O_3)$ ceramics sintered at 1500 °C for 10 min has an average hardness of 1260 HV_1 and a density of 5.73 g/cm^3, respectively, as shown in Table 1. The $ZrO_2(Y_2O_3)$-$30BaCrO_4$ composite sintered at 1100 °C for

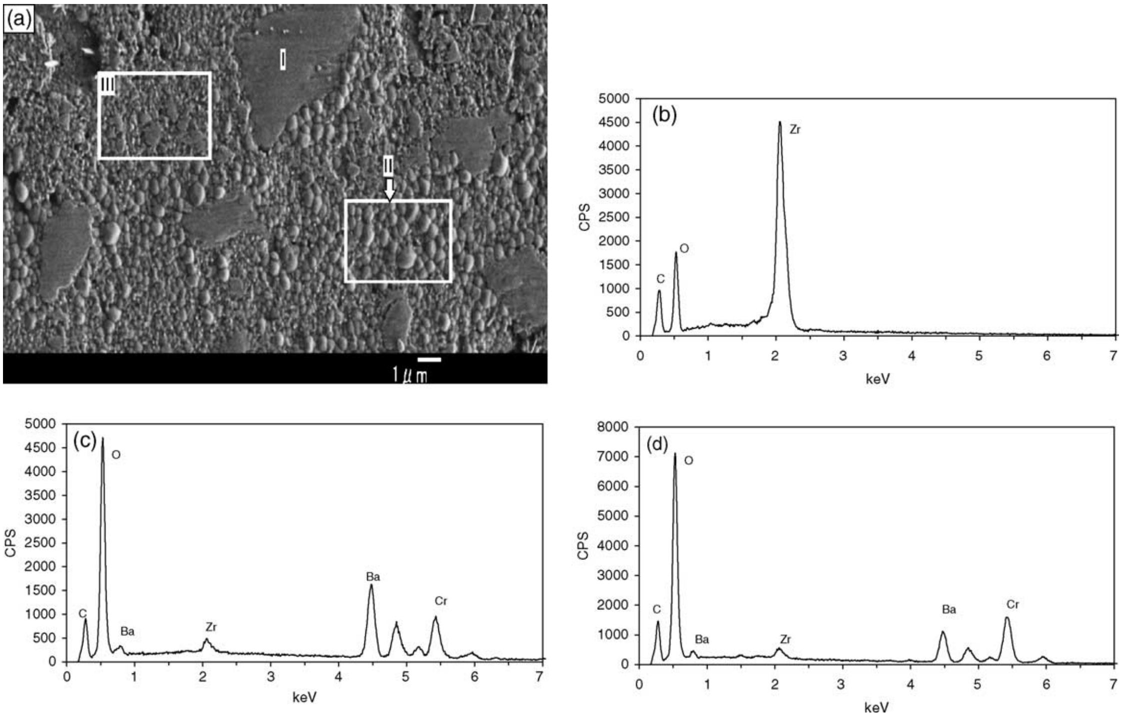

Fig. 1. Microstructure of the $ZrO_2(Y_2O_3)$-$50BaCrO_4$ composite sintered at 1100 °C for 5 min: (a) morphology; (b–d) EDX analyses of different regions (I, II, III) marked in (a).

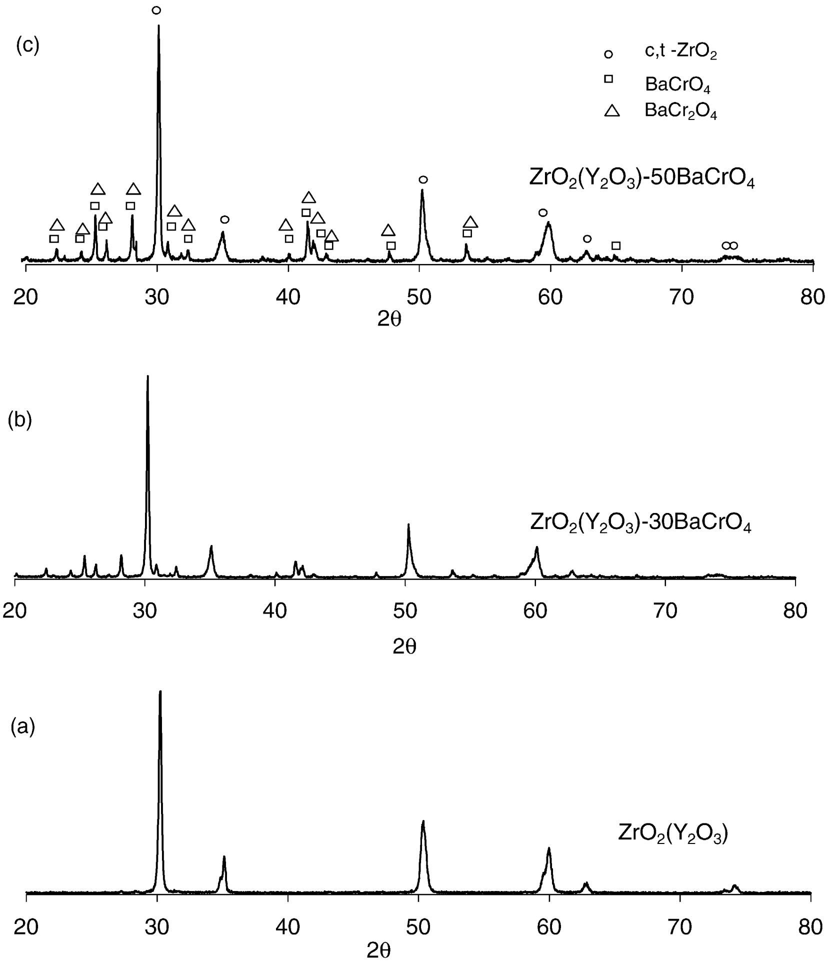

Fig. 2. X-ray diffraction (XRD) spectra of the spark-plasma-sintered composites doped with various amounts of $BaCrO_4$ additive.

5 min has an average hardness of 485 HV_1 and a density of 5.12 g/cm^3. The $ZrO_2(Y_2O_3)$-50$BaCrO_4$ composite sintered at 1100 °C for 5 min exhibits an average hardness of 426 HV_1 and a density of 4.99 g/cm^3. Fig. 1 shows the microstructure of $ZrO_2(Y_2O_3)$-50$BaCrO_4$ composite sintered at 1100 °C for 5 min. The sintering process results in densification of the powder mixture. The EDX analyses in Fig. 1(b–d) illustrate the chemical composition of different regions in the composite. The angular phase marked by I in Fig. 1(a) consists of zirconium and oxygen. The other regions marked by II and III in Fig. 1(a) are mainly composed of barium, chromium and oxygen with small amounts of zirconium. However, the ratio of barium to chromium at these regions is quite different. Relatively stronger chromium peak and weaker barium peak were detected at the region III (Fig. 1(d)) than those at the region II (Fig. 1(c)). The barium chromates in the composite are with different ratios of barium to chromium.

The XRD spectra of spark-plasma-sintered $ZrO_2(Y_2O_3)$ matrix composites doped with various amounts of $BaCrO_4$ additive are given in Fig. 2. The composites of both $ZrO_2(Y_2O_3)$-30$BaCrO_4$ and $ZrO_2(Y_2O_3)$-50$BaCrO_4$ sintered at 1100 °C are composed of c,t-ZrO_2, $BaCrO_4$ and $BaCr_2O_4$ phases. From the appearance, the color is green-yellow on polished surfaces of the sintered samples, which is clearly different from the original $BaCrO_4$ powder (yellow). Sintering at 1100 °C in a graphite mold leads to partial decomposition of $BaCrO_4$ to a low oxygen-containing compound such as $BaCr_2O_4$ with a green color. Both $BaCrO_4$ and $BaCr_2O_4$ exhibit an orthorhombic structure. The $BaCrO_4$ structure has a slightly larger lattice parameter of both a and c, but a slightly smaller value of c/a than the $BaCr_2O_4$ structure. Thermal data of individual $BaCrO_4$ structure showed that the $BaCrO_4$ phase was thermally stable to 850 °C [13], and may decompose into a mixture of $BaCr_2O_4/9BaO{\cdot}4Cr_2O_3{\cdot}CrO_3$ beyond 900 °C according to the phase diagrams of BaO-Cr_2O_3 system [14]. Fig. 3 shows the effect of sintering temperature on the phase structure in the $ZrO_2(Y_2O_3)$-50$BaCrO_4$ composites. When the sintering temperature is at 1150 °C or below, the composite is composed of c,t-ZrO_2, $BaCrO_4$ and $BaCr_2O_4$. The composites exhibit an increase in density and hardness with the increase of temperature over this temperature range as shown in Table 2. However, when the sintering temperature is increased to 1300 °C, chemical reaction between ZrO_2 and $BaCrO_4$ is identified. The phases after chemical reaction

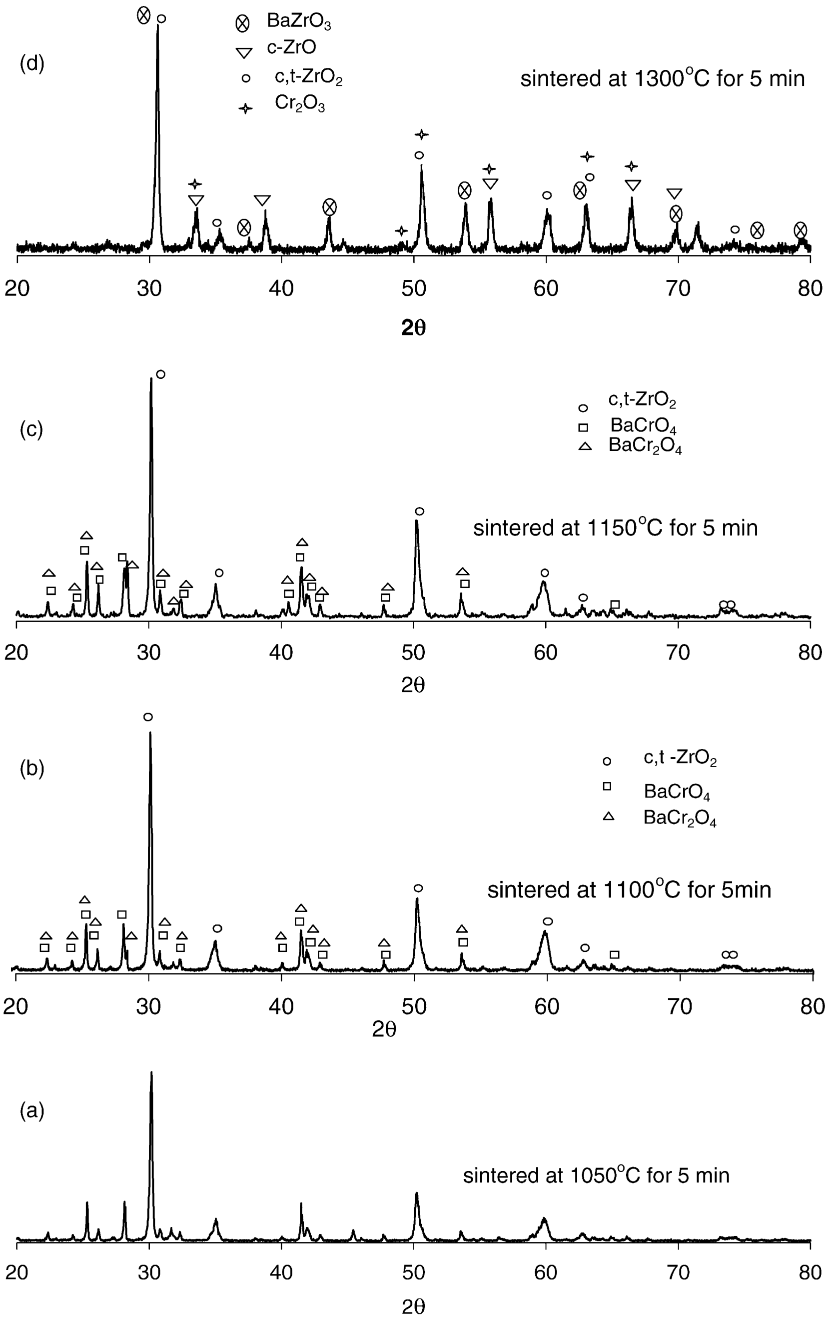

Fig. 3. Effect of the sintering temperature on the phase structure in a $ZrO_2(Y_2O_3)$-50$BaCrO_4$ composite.

are $BaZrO_3$, c,t-ZrO_2, c-ZrO and Cr_2O_3. Some pores are clearly visible in the polished samples. This explains the lower density (4.95 g/cm^3) and lower hardness (389 HV_1) of such composite.

3.2. Friction and wear behavior of $ZrO_2(Y_2O_3)$-$BaCrO_4$ composites and the coupled ball

The effects of $BaCrO_4$ additive on the friction coefficient and wear rate of the spark-plasma-sintered samples and the coupled ball are shown in Fig. 4. The friction coefficient and wear rate of the $ZrO_2(Y_2O_3)$ ceramics rapidly increase with the test temperature and reach the considerable values of respect 1.53 and 9.29 × 10^{-4} mm^3/Nm at above 200 °C in sliding against an alumina ball. The addition of 30 wt.% $BaCrO_4$ in the $ZrO_2(Y_2O_3)$ ceramics clearly improves the friction and wear properties at elevated temperatures as shown in Fig. 4. The friction coefficient and wear rate of the $ZrO_2(Y_2O_3)$-30$BaCrO_4$ composite gradually decrease to 0.56 and 2.64 × 10^{-5} mm^3/Nm at 800 °C. However, its friction coefficient and wear rate at room temperature are 0.71 and 6.12 × 10^{-5} mm^3/Nm, respectively. The wear rates of the coupled ball show similar trends with temperature, but range between 5.13 × 10^{-6} and 3.96 × 10^{-5} mm^3/Nm in

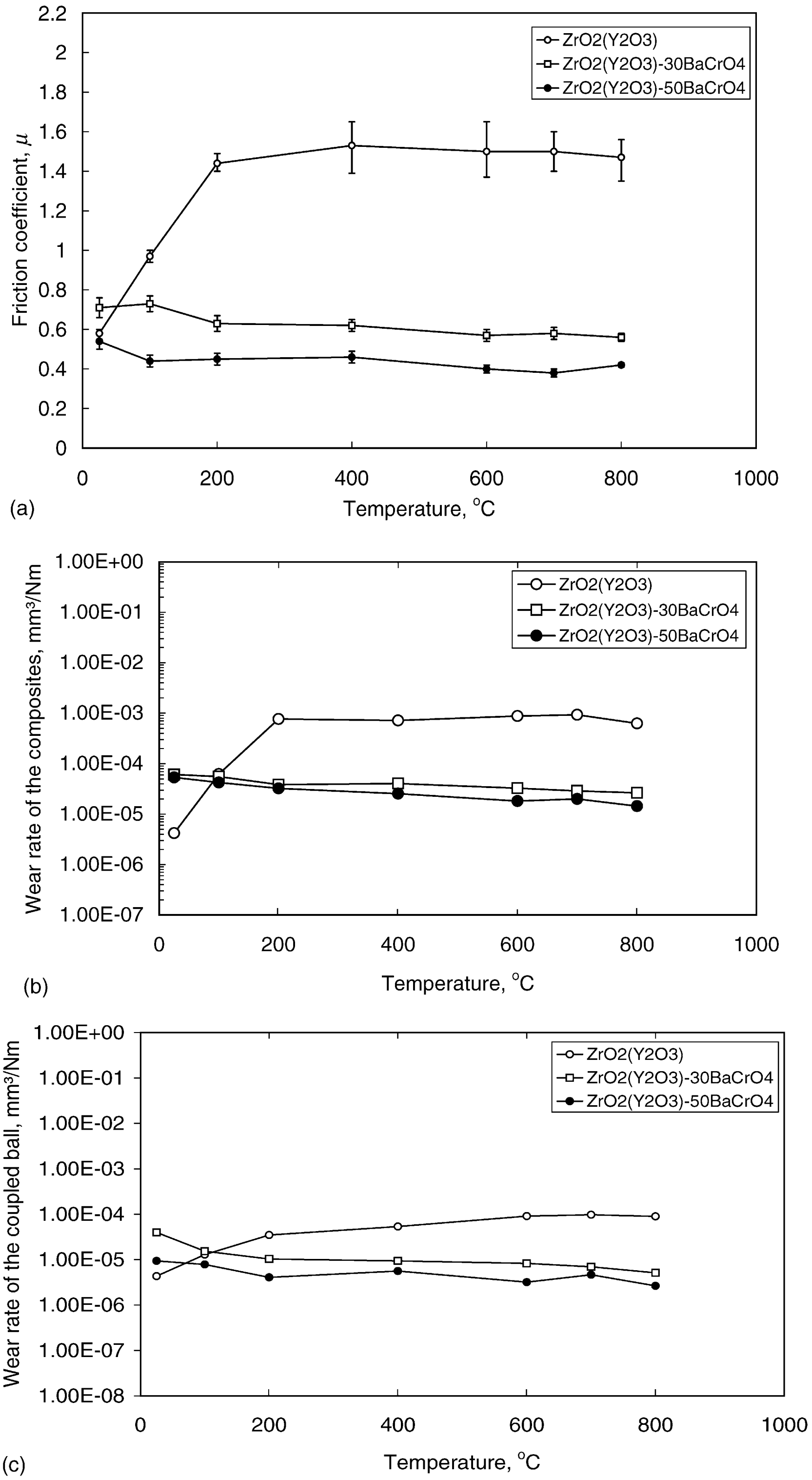

Fig. 4. Effects of $BaCrO_4$ additive on the friction coefficient and wear rate of the spark-plasma-sintered samples and the coupled ball: (a) friction coefficient; (b) wear rate of the composites; (c) wear rates of the coupled ball.

Fig. 4(c). When the content of $BaCrO_4$ lubricant increases from 30 to 50 wt.%, the friction coefficient of the composite/Al_2O_3 sliding pair decreases considerably, while the wear rates of the composite and the coupled ball have the lowest values. The $ZrO_2(Y_2O_3)$-50$BaCrO_4$ composite exhibits a coefficient of friction of 0.55 at room temperature, 0.45 at 200 °C, and remains at the level of 0.4 up to 800 °C with a minimum value of 0.38 at 700 °C. The wear rates of the

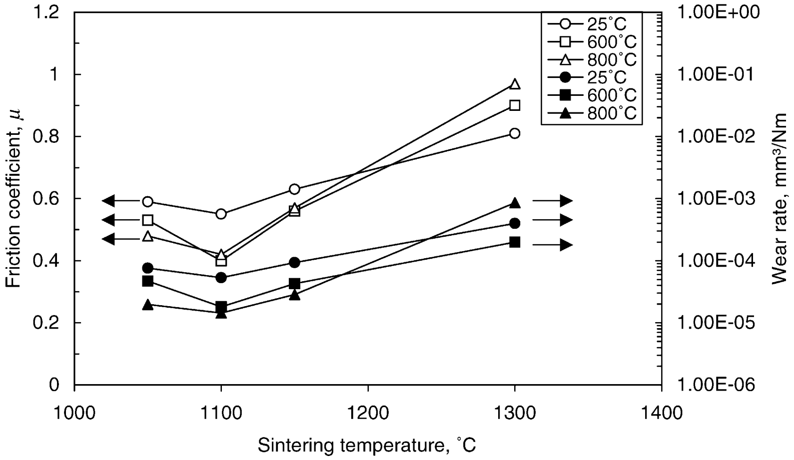

Fig. 5. Effect of the sintering temperature on the friction and wear of the $ZrO_2(Y_2O_3)$-50$BaCrO_4$ composite at different wear test temperatures.

composite are between 1.44×10^{-5} and 5.35×10^{-5} mm^3/Nm as shown in Fig. 4(b). The wear rates of the coupled ball range between 9.33×10^{-6} and 2.65×10^{-6} mm^3/Nm as shown in Fig. 4(c). The friction and wear data indicate that the $ZrO_2(Y_2O_3)$ matrix composite with 50 wt.% $BaCrO_4$ is the most effective in reducing both friction and wear over the entire temperature range investigated.

The effects of the sintering temperature on the friction and wear of the $ZrO_2(Y_2O_3)$-50$BaCrO_4$ composite at different wear test temperatures are illustrated in Fig. 5. The lowest friction coefficient and wear rate over the entire temperature range studied were obtained for the composite sintered at 1100 °C for 5 min. The friction coefficient is between 0.38 and 0.55, while the wear rate of the composite is between 1.44×10^{-5} and 5.35×10^{-5} mm^3/Nm. The composites sintered at 1050 °C or 1150 °C for 5 min exhibit higher friction and wear data than the composite sintered at 1100 °C for 5 min as shown in Fig. 5. Furthermore, the composites sintered at 1300 °C for 5 min have the highest friction coefficient and wear rates under the identical wear conditions. The friction coefficients are over 0.8 at low temperatures, while the wear rates of the composites are unacceptable.

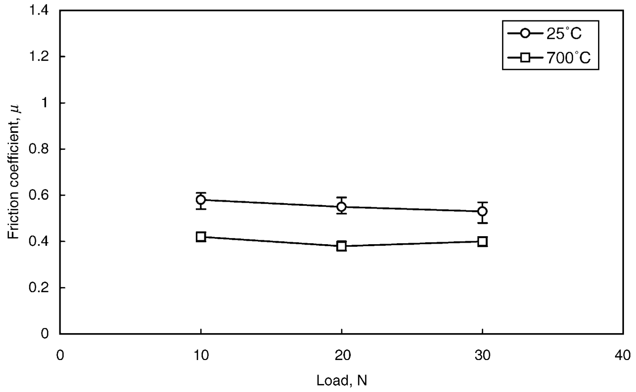

Fig. 6. Effect of load on the friction coefficient of the $ZrO_2(Y_2O_3)$-50$BaCrO_4$ composite at different wear test temperatures.

Further tribological studies at different loads have been performed for the $ZrO_2(Y_2O_3)$-50$BaCrO_4$ composites sintered at 1100 °C for 5 min. The effect of load on the friction coefficient of the $ZrO_2(Y_2O_3)$-50$BaCrO_4$ composite at different wear test temperatures is shown in Fig. 6. It can be seen that the $ZrO_2(Y_2O_3)$-50$BaCrO_4$ composite exhibits relatively stable values in friction with the increase of load from 10 to 30 N. At room temperature, the friction coefficient is relatively high, and ranges between 0.58 at 10 N and 0.53 at 30 N. At 700 °C, the friction coefficient has a relatively low value between 0.38 and 0.42.

3.3. Observations of worn surfaces of selected $ZrO_2(Y_2O_3)$-$BaCrO_4$ composite and the coupled ball

The worn surfaces of selected $ZrO_2(Y_2O_3)$-50$BaCrO_4$ composite sintered at 1100 °C for 5 min and the wear scars of the coupled ball were examined to identify the lubrication mechanisms. The worn surface of the $ZrO_2(Y_2O_3)$-50$BaCrO_4$ composite after room temperature wear test is shown in Fig. 7. Surface brittle fracture is observed on the worn surface in Fig. 7(a). Some fine wear debris and cracks are found in Fig. 7(b) without continuous lubrication film occurring on the worn surface. EDX analysis of the worn surface in Fig. 7(c) demonstrates the presence of a large quantity of zirconium, oxygen and some amounts of barium and chromium. Raman spectrum in Fig. 7(d) shows that the worn surface is composed of zirconia and barium chromates, as compared to the referred spectra (Fig. 7(e and f)) of original $ZrO_2(Y_2O_3)$ and $BaCrO_4$ powders. Clearly, the presence of a large number of zirconia ceramics at the tribo-contact regions leads to surface brittle fracture.

Fig. 8 shows the worn surface of the $ZrO_2(Y_2O_3)$-50$BaCrO_4$ composite after 200 °C wear test. The worn surface becomes relatively smooth. From the enlarged

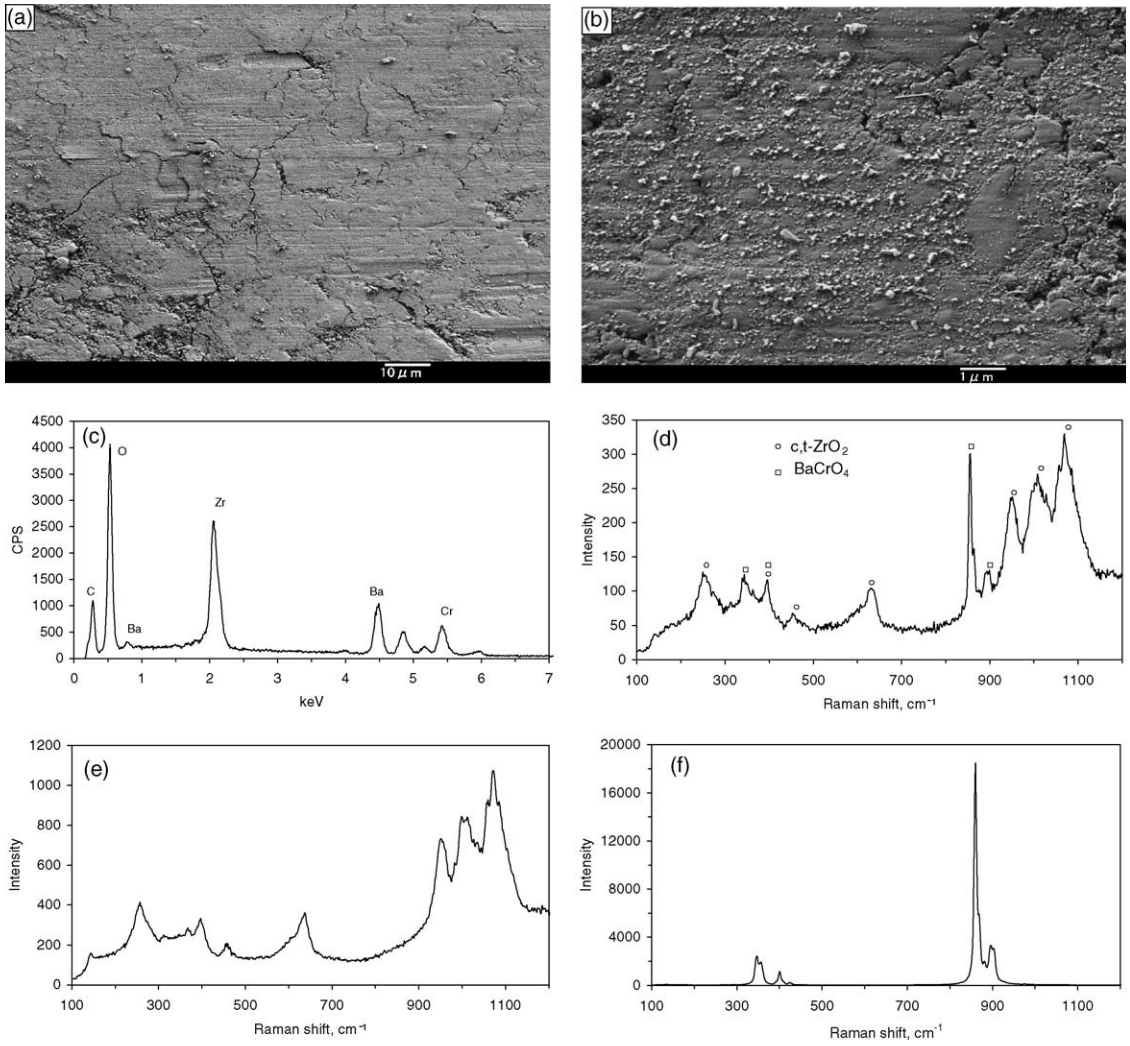

Fig. 7. Worn surface of the $ZrO_2(Y_2O_3)$-50$BaCrO_4$ composite after room temperature wear test: (a) worn surface; (b) enlarged view; (c) EDX analysis of (b); (d) Raman spectrum of the worn surface; (e) and (f) referred spectra of original $ZrO_2(Y_2O_3)$ and $BaCrO_4$ powders.

micrograph in Fig. 8(b), many fine grains are found on the worn surface together with distinct traces of plastic flow. The EDX analysis in Fig. 8(c) reveals that there is distinct compositional difference on tribo-contact surfaces with the increase of temperature. The peaks of barium and chromium become strong, as compared to Fig. 7(c). Raman spectrum in Fig. 8(d) shows the presence of a large number of $BaCrO_4$ on the worn surface. The worn surface exhibits an apparent rise in $BaCrO_4$ content. Surface analyses suggest that the friction and wear will be reduced when the surface is enriched in barium chromates.

The worn surface of the $ZrO_2(Y_2O_3)$-50$BaCrO_4$ composite after 600 °C wear test is shown in Fig. 9. The worn surface of the composite seems to be covered with a discontinuous film as well as with distinct spoors of plastic deformation. An enlarged SEM micrograph in Fig. 9(b) reveals some microcracks and a large number of fine $BaCrO_4$ grains in the wear surface layer, elongated in the sliding direction. The EDX analysis revealed that the worn surface was enriched with $BaCrO_4$, indicating the formation of a discontinuous $BaCrO_4$ grain layer.

The worn surface of the $ZrO_2(Y_2O_3)$-50$BaCrO_4$ composite after 800 °C wear test can be observed in Fig. 10. Almost no wear debris is generated after 800 °C wear test. The worn surface of the composite is very smooth with distinct spoors of plastic deformation. An enlarged micrograph in Fig. 10(b) shows that the worn surface is covered with a deformed fine grain layer. The EDX analysis in Fig. 10 (c) shows that the deformed surface consists mainly of barium, chromium and oxygen with very small amounts of zirconium. Raman spectrum in Fig. 10(d) identified the phase structure on the worn surface is mainly composed of $BaCrO_4$. It suggests that the well-covered fine $BaCrO_4$ grain layer on the worn surface reduce the friction and wear at 800 °C.

At room temperature, the wear scar is very clean, and no detectable transfer product from the composite is found on the wear scar of the coupled ball. Fig. 11 shows the

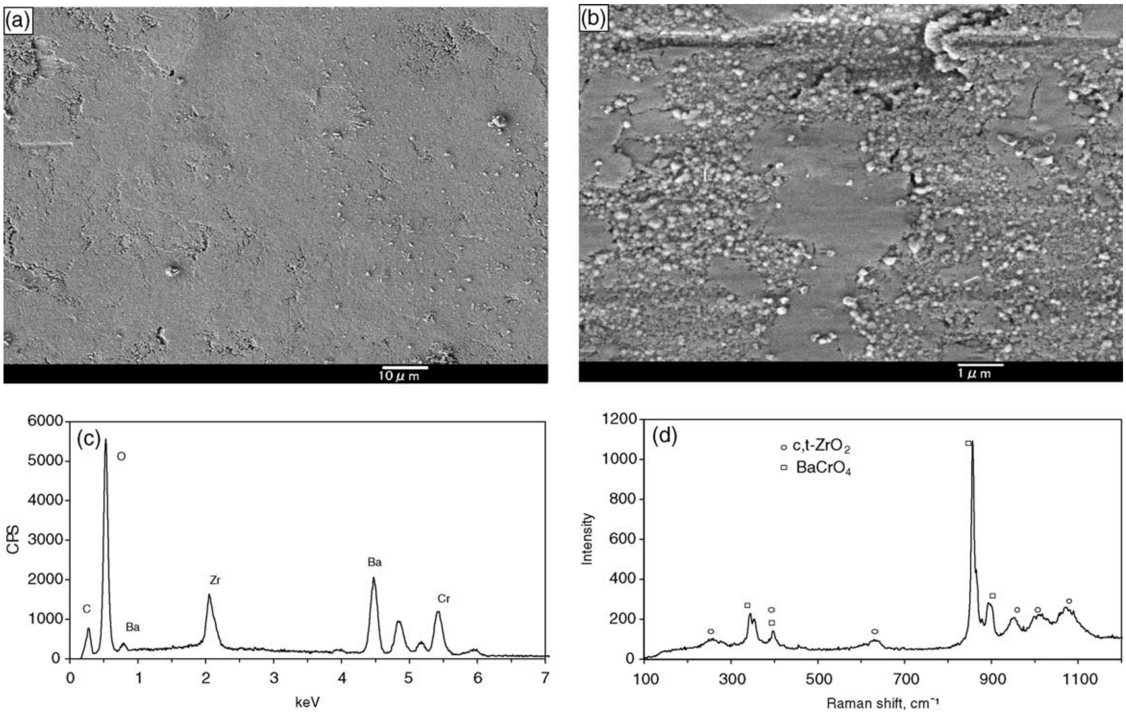

Fig. 8. Worn surface of the $ZrO_2(Y_2O_3)$-50$BaCrO_4$ composite after 200 °C wear test: (a) morphology; (b) enlarged view of (a); (c) EDX analysis of (b); (d) Raman spectrum of the worn surface.

morphology of wear scars on the coupled ball after sliding on the $ZrO_2(Y_2O_3)$-50$BaCrO_4$ composite at different wear test temperatures. The wear scar after 200 °C wear test experiences detectable transfer of $BaCrO_4$ from the composite to the coupled ball. The EDX analysis in Fig. 11(c) shows the presence of barium and chromium, indicating the formation of a discontinuous $BaCrO_4$ transfer layer on the wear scar. From Fig. 11(b), a transfer layer is also found on the wear scar of the coupled ball after 800 °C wear test. The EDX analysis of the wear scar demonstrates that the transferred products contain barium, chromium and oxygen. This verifies that the $BaCrO_4$ constituent is partially built-up on the surface of the coupled ball, and effectively reduces the friction and wear removal of the composite and the coupled ball.

4. Discussion

The spark-plasma-sintered $ZrO_2(Y_2O_3)$-50$BaCrO_4$ composites show promise for sliding wear applications up to 800 °C. The addition of $BaCrO_4$ greatly improves intermediate and high temperature lubricating properties without adversely affecting low-temperature tribological properties, as compared to the unmodified $ZrO_2(Y_2O_3)$ ceramics. The $ZrO_2(Y_2O_3)$-50$BaCrO_4$ composite exhibited a friction coefficient of 0.38 to 0.55 and a wear rate of 1.44×10^{-5} to 5.35×10^{-5} mm^3/Nm up to 800 °C. The wear rates of the coupled ball range between 9.33×10^{-6} and 2.65×10^{-6} mm^3/Nm.

The friction and wear data indicate that the $ZrO_2(Y_2O_3)$-50$BaCrO_4$ composite sintered at 1100 °C exhibits the

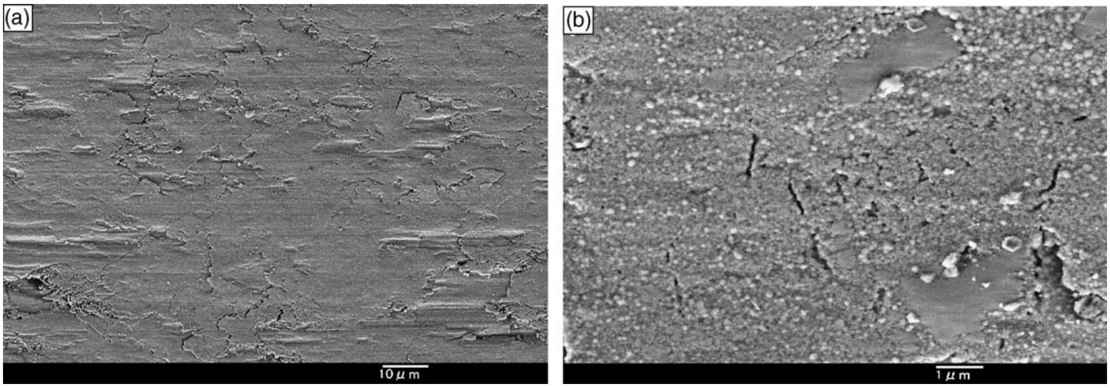

Fig. 9. Worn surface of the $ZrO_2(Y_2O_3)$-50$BaCrO_4$ composite after 600 °C wear test: (a) morphology; (b) enlarged view of (a).

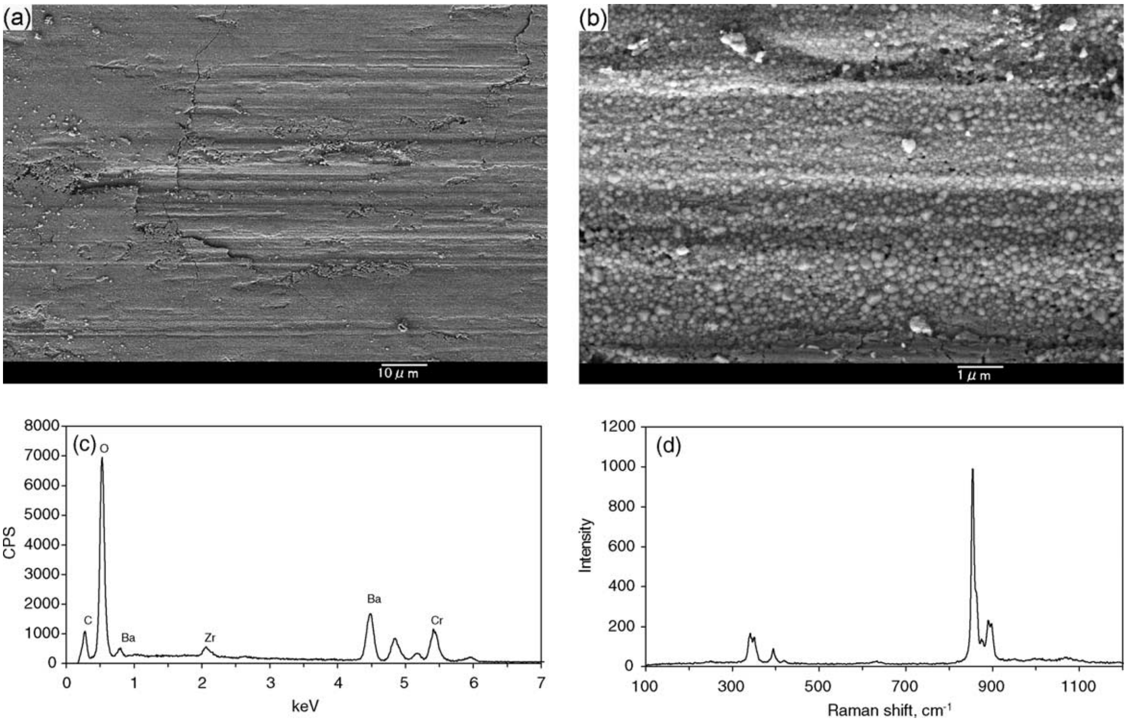

Fig. 10. Worn surface of the $ZrO_2(Y_2O_3)$-50$BaCrO_4$ composite after 800 °C wear test: (a) morphology; (b) enlarged view of (a); (c) EDX analysis of (b); (d) Raman spectrum of the worn surface.

lowest friction coefficients and wear rates over the entire temperature range studied. When the sintering temperature is at 1150 °C or below, the $ZrO_2(Y_2O_3)$-50$BaCrO_4$ composite is composed of c,t-ZrO_2, $BaCrO_4$ and $BaCr_2O_4$. During spark plasma sintering, some original $BaCrO_4$ powders partially decompose into a $BaCr_2O_4$ structure. Both $BaCrO_4$ and $BaCr_2O_4$ exhibit an orthorhombic structure with slightly different lattice parameters, depending on the

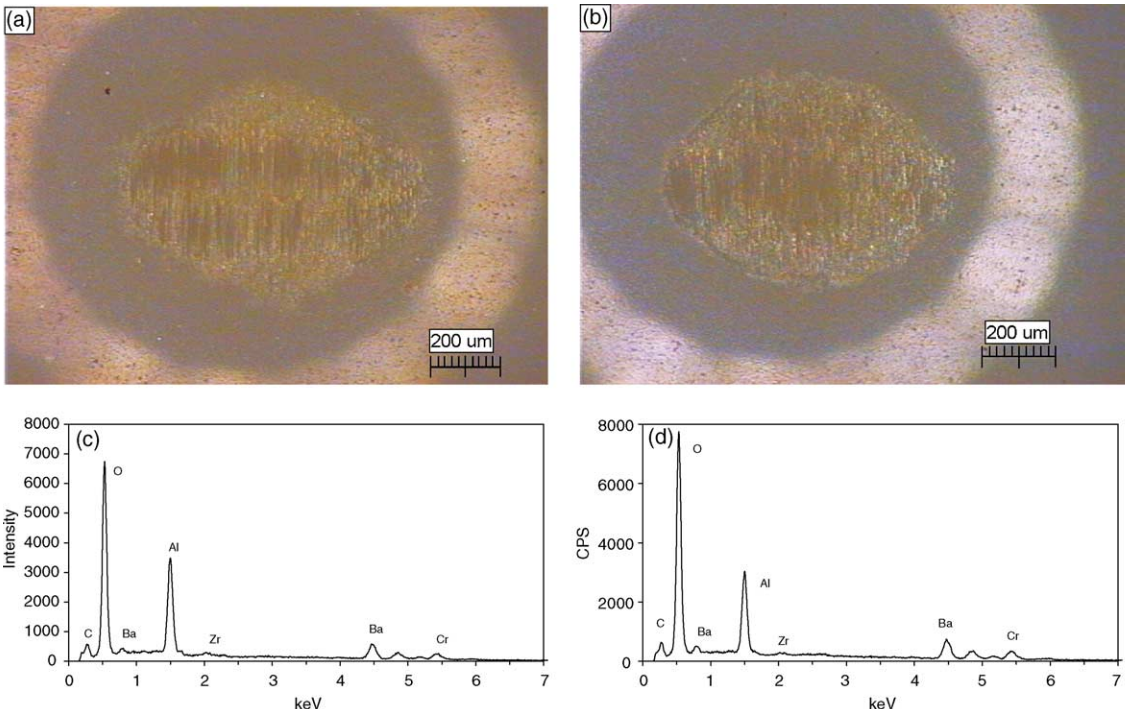

Fig. 11. Wear scars on the coupled ball after sliding on the $ZrO_2(Y_2O_3)$-50$BaCrO_4$ composite at different wear test temperatures: (a) 200 °C; (b) 800 °C; (c) and (d) EDX analyses of the wear scars in (a) and (b).

oxidation degree of compounds. At elevated temperatures, the barium chromates become soft, and further spread out on the worn surface in tribological stressing, creating a self-lubricating fine grain layer in the wear track. The SEM observations indicate an enrichment in fine $BaCrO_4$ grains on the worn surface at high temperatures.

After room temperature wear test, the presence of a large amount of brittle $ZrO_2(Y_2O_3)$ ceramics leads to cracking and material removal in the form of abrasives from the worn surface, and increases friction and wear. Surface brittle fracture is considered as the dominating wear mechanism of the composite at room temperature. After 200 °C wear test, $BaCrO_4$ constituent is partially transferred to the coupled ball, and avoids the direct tribo-contact between the $ZrO_2(Y_2O_3)$ ceramics and alumina. The barium chromate is easily softened at elevated temperatures, and was partially transferred to the counterfaces to effectively reduce friction and wear. The formation of a well-covered $BaCrO_4$ grain layer will prevent severe wear of the composite, due to a transition in wear mechanism from surface brittle fracture to plastic deformation. For self-lubricating $ZrO_2(Y_2O_3)$-50$BaCrO_4$ composites, the formation and effective spreading of $BaCrO_4$ fine grain layer are the most important factor to reduce friction and wear rate over a wide temperature range. Plastic deformation during sliding plays an important role in the formation of a self-lubricating $BaCrO_4$ grain layer on the worn surface. Therefore, barium chromate is considered to be a performing solid lubricant in composite materials for tribological applications up to 800 °C in air.

5. Conclusions

(1) The addition of $BaCrO_4$ greatly improves intermediate and high temperature lubricating properties without adversely affecting low-temperature tribological properties, as compared to the unmodified $ZrO_2(Y_2O_3)$ ceramics. The $ZrO_2(Y_2O_3)$-50$BaCrO_4$ composite exhibited a friction coefficient of 0.38 to 0.55 and a wear rate of 1.44×10^{-5} to 5.35×10^{-5} mm^3/Nm up to 800 °C. The wear rates of the coupled ball range between 9.33×10^{-6} and 2.65×10^{-6} mm^3/Nm.

(2) Surface brittle fracture is considered as the dominating wear mechanism of the composite at room temperature. At elevated temperatures, a self-lubricating $BaCrO_4$ fine-grain layer formed on the worn surfaces, and was partially transferred to the counterface to effectively reduce friction and wear. Plastic deformation during sliding plays an important role in the formation of a well-covered fine grain layer of $BaCrO_4$ on the tribo-contact regions.

(3) When the sintering temperature is at 1150 °C or below, the $ZrO_2(Y_2O_3)$-50$BaCrO_4$ composite is composed of c,t-ZrO_2, $BaCrO_4$ and $BaCr_2O_4$. However, when the sintering temperature is increased to 1300 °C, the composite consists of $BaZrO_3$, c,t-ZrO_2, C-ZrO and Cr_2O_3. The friction and wear data indicate that the composite sintered at 1100 °C exhibits the lowest friction coefficients and wear rates up to 800 °C.

References

[1] H.E. Sliney, Solid lubricant materials for high temperatures: a review, Tribol. Int. 15 (1982) 303–315.

[2] C. Dellacorte, J.A. Fellenstein, The effect of compositional tailoring on the thermal expansion and tribological properties of PS300: a solid lubricant composite coating, Tribol. Trans. 40 (4) (1997) 639–642.

[3] Y. Jin, K. Kato, N. Umehara, Further investigation on the tribological behavior of Al_2O_3–20Ag20CaF_2 composite at 650 °C, Tribol. Lett. 6 (1999) 225–232.

[4] J.H. Ouyang, S. Sasaki, K. Umeda, Low-pressure plasma-sprayed ZrO_2–CaF_2 composite coating for high temperature tribological applications, Surf. Coat. Technol. 137 (2001) 21–30.

[5] J.H. Ouyang, S. Sasaki, K. Umeda, Microstructure and tribological properties of low-pressure plasma-sprayed ZrO_2–CaF_2–Ag_2O composite coating at elevated temperature, Wear 249 (2001) 440–451.

[6] J.H. Ouyang, S. Sasaki, Effects of different additives on microstructure and high-temperature tribological properties of plasma-sprayed Cr_2O_3 ceramic coatings, Wear 249 (2001) 56–67.

[7] S. Sasaki, Tribological evaluation of plasma sprayed coatings for high temperature sliding surface against cordierite, Mater. Manuf. Process. 14 (2) (1999) 185–194.

[8] T.A. Blanchet, J.H. Kim, S.J. Calabrese, C. Dellacorte, Thrust-Washer evaluation of self-lubricating PS304 composite coatings in high temperature sliding contact, Tribol. Trans. 45 (4) (2002) 491–498.

[9] C. Dellacorte, H.E. Sliney, Composition optimization of self-lubricating chromium-carbide based composite coatings for use to 760 °C, ASLE Trans. 30 (1) (1987) 77–83.

[10] J.H. Ouyang, S. Sasaki, K. Umeda, The friction and wear characteristics of low-pressure plasma-sprayed ZrO_2–$BaCrO_4$ composite coating at elevated temperatures, Surf. Coat. Technol. 154 (2002) 131–139.

[11] K. Umeda, A. Tanaka, S. Takatsu, Development of multi-oxide solid lubricants usable from room temperature up to 1000 °C, International Tribology Conference, 29 October–2 November 1995, in: Proceedings of the International Tribology Conference, The Japanese Society of Tribologists, Yokohama, Japan, vol. 2, 1996, pp. 1181–1186.

[12] S. Nuzeki, T. Yoshioka, H. Mizutani, H. Kotorii, H. Toyota, T. Hashimoto, H. Kashimura, M. Takamori, H. Sugi, E. Hirai, Solid lubricants for high temperature ceramic rolling bearings (part 1)—various solid lubricants based on fluoride compounds, J. Mech. Eng. Lab. 49 (3) (1995) 84–95 (in Japanese).

[13] R.M. Gabr, A.M. El-Award, M.M. Girgis, Physico-chemical and catalytic studies on the calcinations products of $BaCrO_4$–CrO_3 mixture, Mater. Chem. Phys. 30 (1992) 253–259.

[14] A.M. Azad, R. Sudha, O.M. Sreedharam, The standard Gibbs energies of formation of $ACrO_4$ (A = Ca, Sr or Ba) from EMF measurements, Thermochim. Acta 194 (1992) 129–136.